

RSC Advances

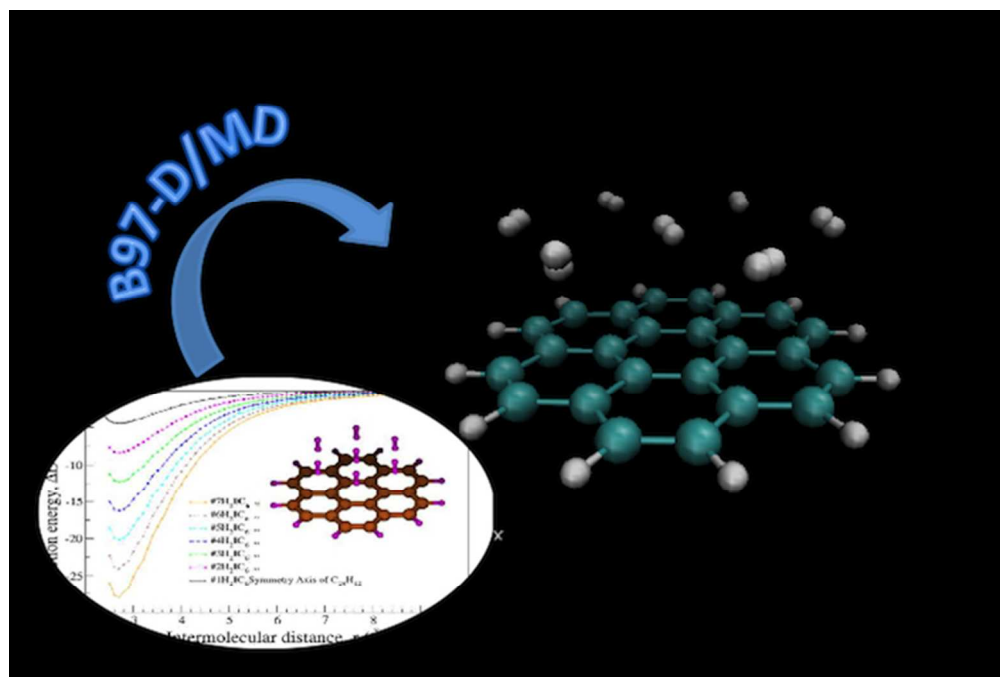


This is an *Accepted Manuscript*, which has been through the Royal Society of Chemistry peer review process and has been accepted for publication.

Accepted Manuscripts are published online shortly after acceptance, before technical editing, formatting and proof reading. Using this free service, authors can make their results available to the community, in citable form, before we publish the edited article. This *Accepted Manuscript* will be replaced by the edited, formatted and paginated article as soon as this is available.

You can find more information about *Accepted Manuscripts* in the [Information for Authors](#).

Please note that technical editing may introduce minor changes to the text and/or graphics, which may alter content. The journal's standard [Terms & Conditions](#) and the [Ethical guidelines](#) still apply. In no event shall the Royal Society of Chemistry be held responsible for any errors or omissions in this *Accepted Manuscript* or any consequences arising from the use of any information it contains.



59x40mm (300 x 300 DPI)

Multiscale modelling and simulation (MMS) combining B97-D/TZV2P DFT calculations and Molecular Dynamics simulations are performed to investigate the adsorption of hydrogen over coronene as a model of graphene

Multi-scale Theoretical Investigation of Molecular Hydrogen Adsorption over Graphene: Coronene As a Case Study

Md Bin Yeamin,^a N. Faginas-Lago^{*b‡} M. Albertí,^c I. G. Cuesta,^a J. Sánchez-Marín^a and A. M. J. Sánchez de Merás^{*a‡}

Received Xth XXXXXXXXXXXX 20XX, Accepted Xth XXXXXXXXXXXX 20XX

First published on the web Xth XXXXXXXXXXXX 200X

DOI: 10.1039/b000000x

The physisorption of molecular hydrogen onto coronene is studied using a multi-scale theoretical approach with Density Functional Theory (DFT) calculations and Molecular Dynamics (MD) simulations. We consider two different kinds of model conformations for the approach of hydrogen towards the coronene i.e., systematic and random. For the systematic attack of hydrogen over coronene, the resulting potential energy profiles from DFT analysis are further found resembling to the Morse potential, and even to the largely flexible Murrell-Sorbie (M-S) potential. The resulting M-S fitting also shows a zero-point energy correction of ~ 16 - 17 %. On the other hand, the potential energies from the random approach has been implemented into the Improved Lennard-Jones (ILJ) force field of DL_POLY package following a prior statistical treatment. The MD simulations have been performed at different temperatures from 10 to 390 K. For the interaction of seven hydrogen molecules with coronene, the DFT method shows an average interaction energy of -3.85 kJ/mol per H_2 , which is standing slightly below the Coupled Cluster value (CCSD(T)) of -4.71 kJ/mol that was calculated for a single molecule in the most favorable situation. Moreover, the MD calculations reveal a mean interaction energy of -3.69 kJ/mol per H_2 (a gross mean $E_{c,fg}$ of -25.98 kJ/mol at $T = 299.97$ K), which is again in good agreement to the aforementioned DFT results, proving the quality of the used approach for the study of van der Waals interactions between hydrogen and graphene.

1 Introduction

Hydrogen energy has received an impressive attention towards the future post-petroleum ages as an alternative clean energy, since the reservation of fossil fuels is decreasing with the growing consumer demand. Hydrogen is the most abundant element in the Universe, mainly in stars. Although molecular hydrogen does not occur on the earth in significant amount, it can be extracted decomposing water by using chemical, thermal or electrical energy and from renewable resources like biomass or coal by some consecutive natural processes. In this context, the proper use of hydrogen makes its storage a crucial issue along with other branches of the hydrogen technology progress^{1,2} and, therefore, a considerable amount of work has been dedicated to the search for the efficient and technology-friendly hydrogen storage materials. Several materials have significant hydrogen storage capacity, as for instance porous materials, different kinds of hydrides and

carbonaceous nanomaterials.³ In particular, the potential use of graphene for gas sensing has attracted attention of the scientific community in the last years,⁴⁻⁹ being considered a good candidate for gas storage^{1,2}.

Graphene, with its honeycomb two-dimensional structure of sp^2 carbon atoms, is with no doubt one of the most important materials to be investigated¹⁰⁻¹² because of its robustness, flexibility and enormous surface area. Furthermore, the capability of graphene to adsorb different gases is also important from an environmental point of view.¹³ It could be used to store CH_4 ^{14,15} or CO_2 ^{13,16} in order to prevent global warming caused by greenhouse gases. Nevertheless, so far, the storage capacity obtained at room temperature and pressure is still far away from the target of US Department of Energy (DoE), which is 9.0 wt% gravimetric density and 81 g L^{-1} volumetric capacity by 2015.¹⁷ Anyway, from a technological point of view, graphene provides an ideal environment to investigate catalytic processes, surface diffusion and molecular hydrogen formation from chemisorbed atomic hydrogen.¹⁸

The interaction of atomic and molecular hydrogen with graphene has been investigated from theoretical and experimental point of views.¹⁹ The physisorption of molecular hydrogen on models of planar and curved graphenes has been

^a Instituto de Ciencia Molecular, Universidad de Valencia, Valencia (Spain); E-mail: sanchez@uv.es

^b Dipartimento di Chimica, Biologia e Biotecnologie, Università di Perugia, Perugia (Italy). Fax: +39 075 585 5606; Tel: +390 075 585 5527; E-mail: pivro@gmail.com

^c IQTCUB, Departament de Química Física, Universitat de Barcelona, Barcelona (Spain).

‡ These authors contributed equally to this work

reported by Okamoto *et al.*,²⁰ Vilaplana,²¹ and Patchkovskii *et al.*,²² among others. The main conclusions of those works are the importance of the availability of accurate C-H₂ potentials and the fact that among the three possible adsorption sites (hollow, bridge and on-top sites) the interaction is most attractive at the hollow sites. MD studies on the adsorption and desorption behavior of hydrogen on graphites have also been reported recently.^{16,23}

Today, multiscale modeling and simulation (MMS) is considered as a prominent methodological approach in computational science and engineering.²⁴ The usual strategy of MMS is to apply the more accurate and expensive results from the first-principle Density Functional Theory (DFT) calculations to the atomic and/or molecular scale force fields (inexpensive but less accurate) of classical simulations such as Molecular Dynamics (MD), Monte Carlo (MC), Molecular Mechanics (MM) etc., for a particular model chemical system. For gas-solid system, the first-principle calculations investigate the gas adsorption behaviors such as specific adsorption sites, binding energies, and interaction mechanisms. In the counterpart, MD simulations explore the dynamic properties of the system, which subsequently produce the simulated macroscopic gas adsorption properties for the modeled material in order to complement experimental work.

In the last years, it has been proposed a modification of the Lennard Jones potential energy, the Improved Lenard Jones (ILJ),^{25,26} useful to describe both bonded²⁷ and nonbonded (see for instance refs.^{28,29}) non-electrostatic interaction contributions. The model contains only one additional parameter with respect to the LJ function but it is sufficient to add flexibility and to improve the description of the interaction at both long and short range simultaneously. The parameters of the interaction can be obtained by assuming the additivity of the bond polarizabilities but in the present investigation we are interested in using the ILJ model to fit the DFT computation.

Our purpose in this investigation is to carry out a theoretical study on the adsorption of molecular hydrogen on coronene (C₂₄H₁₂), which can be considered a good prototype for graphene. To this end, the interaction of coronene with up to seven hydrogen molecules in different geometrical conformations has been analyzed at the DFT level of theory. After that, the obtained results has been fitted to an analytical function and the adsorption investigated by means of Molecular Dynamics (MD) simulations.

The paper is structured as follows: in section 2 the results of our first principles calculations are collected. In section 3, we

outline the formulation of the semiempirical PES (potential energy surface) and in section 4, the results of MD simulations are presented. The most important conclusions are given in section 5.

2 First Principles calculations

The geometry of coronene was optimized at the B3LYP/6-31G** level^{30,31} of DFT on Gaussian09 package³². Then, the physisorption of molecular hydrogen onto C₂₄H₁₂ has been studied by means of a supermolecular approach correcting BSSE by the counterpoise procedure³³. The interaction energy of this closed-shell system was computed using B97-D functional³⁴ and split-valence triple-zeta basis supplemented with two polarization functions TZV2P.³⁵ The B97-D functional recovers the attractive dispersion forces through its empirical dispersion term whereas the use of TZV-type basis sets has also been found sufficient to represent the polarization effects in similar systems.³⁶

As a first step, the systematic approach of n molecules of H₂ parallel to the C₆ symmetry axis of coronene was investigated, with n ranging from 1 to 7. In all the cases, one H₂ molecule attacked the center of the coronene, while the remaining ones attacked the center of an outer benzenic hexagons, and when several conformations were allowed, all of them were considered and subsequently averaged. The obtained results are depicted in Figure 1, where the total interaction energy is represented vs. distance for the different number of hydrogens (denoted as # n H₂) approaching perpendicularly to coronene.

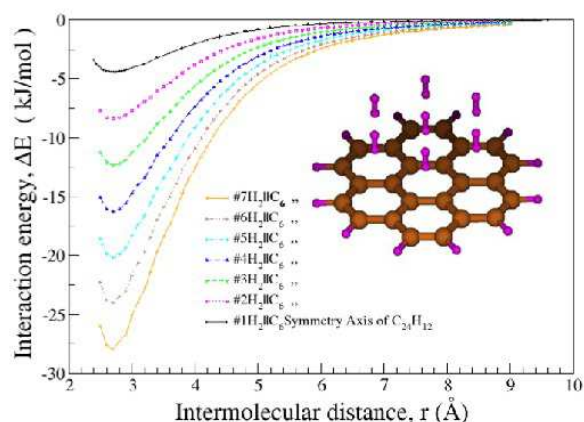


Fig. 1 Mapping of potential energy curves for the adsorption of different number of molecules of H₂ approaching coronene parallel to the C₆ symmetry axis. Distances are measured with respect to the closest hydrogen atom of the H₂ molecule to the coronene surface.

In order to interpret these profiles better, we find it con-

venient to fit the computed values of the interaction energy per hydrogen molecule ΔE to a Murrell-Sorbie³⁷ potential of fourth degree

$$\Delta E = D_e(1 + a_1(r - r_e) + a_2(r - r_e)^2 + a_3(r - r_e)^3 + a_4(r - r_e)^4) \exp(-a_1(r - r_e)) \quad (1)$$

which, because of its larger flexibility, generally provides better results than the well-known Morse potential.

$$\Delta E = D_e(1 - \exp(-a(r - r_e)))^2 \quad (2)$$

From the second derivative at $r = r_e$ of the potential, the constant of the $C_{24}H_{12} - H_2$ van der Waals bond, k , was computed and from it the true dissociation energy, $D_0 = D_e - E_0$, where E_0 is the zero point energy. The determined parameters are collected in Table 1.

Table 1 Parameters (see text for details) from the Murrell-Sorbie fitting of the average energy per hydrogen of different model adsorption systems in systematic adsorption of H_2 over coronene. r_e refers to the distance between the center of mass of H_2 and the coronene surface.

# H_2	$r_e/\text{\AA}$	$D_e/\text{kJ mol}^{-1}$	$k/\text{N m}^{-1}$	$E_0/\text{kJ mol}^{-1}$	$D_0/\text{kJ mol}^{-1}$
1	3.092	4.41	1.77	0.73	3.68
2	3.085	4.15	1.47	0.66	3.49
3	3.079	4.06	1.43	0.65	3.41
4	3.074	4.02	1.42	0.65	3.36
5	3.065	3.98	1.39	0.64	3.33
6	3.057	3.96	1.38	0.64	3.31
7	3.050	3.94	1.37	0.64	3.30

The analysis of Table 1 clearly reveals how the addition of extra hydrogens is weakening the average bond between each hydrogen and the coronene surface. This phenomenon is observed in all the computed parameters since the different energies and the constant of strength of the bond consistently decrease while the bond length increases when enlarging the number of hydrogen molecules. Remarkably, these effects are specially important after adding the second hydrogen molecule. Nevertheless, with the only exception of the adsorption of a single hydrogen molecule, the zero point energy E_0 remains almost constant. Moreover, it is worth to stress that both D_e and D_0 approach to a constant value since the slope of the curve (see Figure 2) is obviously diminishing.

To confirm our previous results, we have also fitted our data to a Morse potential³⁸, getting almost identical results to those reported using Murrell-Sorbie potential again with the only exception of the adsorption of a single hydrogen

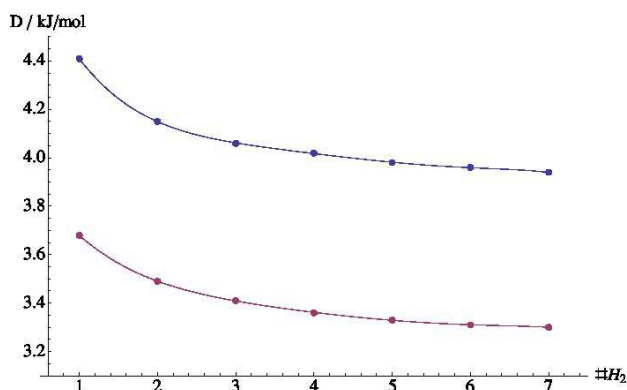


Fig. 2 D_0 (red) and D_e (blue) dissociation energies per molecule as a function of the number of H_2 molecules.

molecule.

At any rate, the parallel conformations considered until now –although useful for a better understanding– are evidently too idealized, as they are extremely improbable. Therefore it is adequate to consider more realistic conformations of the system. To this end, we have randomly generated 99 conformations for each distance between the center of mass of the hydrogen molecules and the coronene surface, and averaged them. In this way, the effects of orientation and position of the H_2 's is accounted for. As one can see in Figure 3, the interaction energy is lowered while the bond distance is enlarged as expected. These facts are also evident in the data presented in Table 2. Furthermore, for the case of seven molecules of hydrogen it can be observed a diminution of the harmonic frequency, ν_e , reflecting the diminution of the bond strength. However, the first anharmonic correction, $x_e \nu_e$ remains almost unaltered in all the cases.

Table 2 Spectroscopic parameters for the adsorption of 1 or 7 H_2 molecules over coronene in parallel and random approaches. r_e indicates the distance between the center of mass of H_2 and the coronene surface.

Approach	$r_e/\text{\AA}$	$D_e/\text{kJ mol}^{-1}$	ν_e/cm^{-1}	$x_e \nu_e/\text{cm}^{-1}$
Parallel_1	3.09	368.6	122.2	0.58
Parallel_7	3.05	329.2	107.4	0.57
Random_1	3.57	318.1	129.6	0.64
Random_7	3.59	271.4	99.4	0.59

In Section 3, the DFT results are utilized to fit a different potential well suited for MD simulations, for using DFT data should improve the performance of such simulations by providing it with a better description of the interaction both at short and long distances.

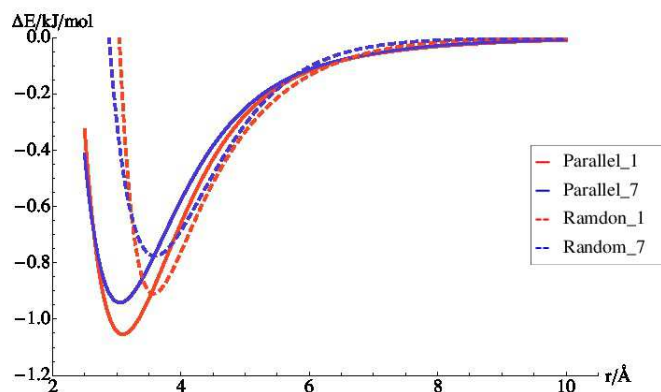


Fig. 3 Comparison of the parallel (continuous lines) and random (dashed lines) approaches of one (red) and seven (blue) hydrogen molecules to coronene.

3 The potential energy surface

The potential model assumes that the total interaction energy from coronene and molecular hydrogen, V_{total} , can be expressed as a sum of interactions involving the hydrogen molecules and the carbon atoms of coronene. Accordingly,

$$V_{total} = \sum_{i=1}^{24} \sum_{j=1}^n V_{C_i-(H_2)_j} + \sum_{j=1}^{n-1} \sum_{k>j}^n V_{(H_2)_j-(H_2)_k} \quad (3)$$

Any V_{C-H_2} and $V_{H_2-H_2}$ term is expressed by means of the ILJ function^{25,26} as,

$$V_{ILJ}(r) = \varepsilon \left[\frac{m}{n(r)-m} \left(\frac{r_0}{r} \right)^{n(r)} - \frac{n(r)}{n(r)-m} \left(\frac{r_0}{r} \right)^m \right] \quad (4)$$

with,

$$n(r) = \beta + 4.0 \left(\frac{r}{r_0} \right)^2 \quad (5)$$

where β is an adjustable parameter related to the hardness of the interacting partners, which adds flexibility to the potential energy function in comparison with the Lennard Jones one. The variable r represents the distance from C atom to the center of mass of the hydrogen molecules for the V_{C-H_2} interactions or the distance between the center of mass of two hydrogen molecules for the $V_{H_2-H_2}$ ones. The m parameter is taken equal to 6, the typical value for neutral-neutral interactions. The well depth ε and the equilibrium distance r_0 have been derived from the DFT results for different values of the β parameter. The advantages of using the ILJ function instead of the LJ one have been well explained elsewhere.²⁵ In order to obtain the best parameters of the potential function for V_{C-H_2} , three statistical treatments are considered:

1. Random averaged (RA): The 99 random conformations of one hydrogen molecule and the coronene are averaged to a H_2 molecule moving along the C_6 axis of coronene. Therefore, the interaction graphene — hydrogen, $V_{C_{24}H_{12},H_2} = \sum_{i=1}^{24} \sum_{j=1}^n V_{C_i-(H_2)_j}$, reduces because of symmetry reasons to the simple form $6V_c + 6V_m + 12V_f$, where V_c , V_m and V_f stand for the interactions with the three symmetric types of carbon atoms (close, medium and far, respectively).
2. Random not averaged (RNA): There is no averaging of the configurations of adsorption interactions. So, for each of the 24 carbon atoms of the coronene structure, there are a total of 2178 C-H atom-atom interactions, resulting from 99 interactions at 22 distances, fitted to the general formula of the ILJ potential according to equation 4.
3. Random not averaged selected (RNA-S): The fitting is also done as in the case above, but with the difference that, in this case, we only include the points near the average value for each distance *i.e.*, those in the interval $\bar{x} \pm \sigma$.

As the final goal of these fittings is to study the interaction of H_2 with graphene, the dangling H atoms of coronene have not been included in any of the fittings. The obtained parameters of the potential defining the interaction between the center of mass of one hydrogen molecule and one C atom of coronene are given in the first part of Table 3.

Table 3 The well depth (ε), the equilibrium distances (r_0) and the β parameter for the C– H_2 and H_2 – H_2 interactions obtained by fitting the DFT results as discussed in text.

Averaged data set	$\varepsilon / \text{kJ mol}^{-1}$	$r_0 / \text{\AA}$	β
C– H_2			
RA	0.289	3.987	8.824
RNA	0.381	3.519	7.295
RNA-S	0.373	3.561	6.777
H_2 – H_2			
RNA	0.406	3.540	6.5

The H_2 - H_2 interaction has also been calculated according to the RNA scheme, representing each hydrogen molecule only by its center of mass. The optimized ILJ parameters are given in the last line of Table 3. Finally, the fitted ILJ function, $V_{C_{24}H_{12},H_2}$, as obtained from the RNA data set of the DFT computation, is represented in Figure 4.

4 Molecular Dynamics simulations

Bearing in mind a posterior study on the adsorption dynamics of molecular hydrogen in graphene, and in order to test the potential parameters, MD simulations of the coronene–(H_2)₇

prototype system have been performed, using the DL_POLY program,³⁹ and considering the microcanonical ensemble (NVE) of particles.

The coronene compound has been kept rigid in all calculations. A time step of 1 fs has been used in all the simulations presented here, integrating the MD trajectories up to final time of 3.5 ns. The time step chosen is large enough to keep the fluctuations of E_{total} well below 10^{-5} kJ mol⁻¹. The MD simulations are preceded by an initial equilibration period of 0.5 ns (using the same time step) during which the velocities of all atoms are rescaled to match the input temperature. The equilibration period has been excluded from the statistical analysis at the end of any trajectory.

In order to decide which set of potential parameters –derived from the three different statistical basis sets considered– is the best one, preliminary MD simulations have been performed using the three sets of parameters. It has been found that the mean values of the potential energy attained along the 3.5 ns of simulation, represented by E_{cfg} (configurational energy) are somewhat different. At a mean temperature of 299.97 K it has been observed that the values of E_{cfg} for $\beta = 7.295$ (RNA data set) is close to that of $\beta = 6.777$ (RNA-S data set). Moreover, it has been found that a better convergence of the total energy is attained when using the potential parameters associated with the RNA data set. Accordingly, we have chosen the parameters given in the third row of Table 3 to calculate the C-H₂ (see Figure 4) interaction and to study the adsorption of molecular hydrogen on coronene.

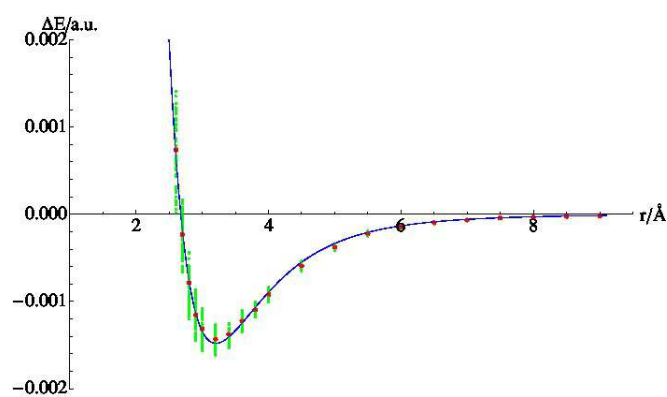


Fig. 4 Fitted ILJ potential (the blue curve) with the averaged interaction energies (the red points) for the coronene-(H₂) system. Moreover, the green points, which accumulate to a bar or to large point, are evaluating the closeness to normal distribution

The quality of the potential parameters has been tested by performing MD simulations at low temperatures of the

coronene with two molecules of H₂ adsorbed. The MD results at the lowest value of temperature investigated are compared with the counterpoise-corrected CCSD(T) results as shown in Table 4. As it can be seen, the MD results are in good agreement with the CCSD(T) ones. The two methods give very similar values of E_{cfg} ($\Delta E_{cfg} = 0.97$ kJ mol⁻¹). This should indicate that the potential parameters are adequate to investigate the adsorption of H₂ on coronene.

Table 4 Lowest distance from the center of mass of the adsorbed molecules to the coronene surface and configurational energy (E_{cfg}) for the coronene-(H₂)₂ system.

Type of calculation	Distances / Å	E_{cfg} / kJ mol ⁻¹
CCSD (T)	3.020	-9.43
	3.020	
MD (T=9.99 K)	3.054	-8.46
	3.046	

The adsorption of seven molecules of H₂ on coronene have been investigated by increasing the temperature from 10 K to 390 K. Results of NVE simulations indicate that the configuration energy, E_{cfg} , remains almost constant ($E_{cfg} \approx -26$ kJ mol⁻¹), which indicates the stability of the system along the temperature change in the mentioned range. Accordingly, the increase of the kinetic energy (due to the increase of T) originates a decrease of the total energy. In order to analyze if any adsorption takes place, we have adopted the same criteria found from the Murrell-Sorbie and Morse potential fittings of the DFT calculation, which establish that adsorption occurs at a distances lower than 3.2 Å from the hydrogen molecules to the C atoms of coronene. Previously, the radial distribution function, RDF, between the center of mass of H₂ and the C atoms has also been analyzed (see Fig. 5). From the figure it seems that the distance criterion mentioned before is adequate for MD simulations.

The results of the MD simulations show that the number of adsorbed molecules changes, depending on the initial configuration and temperature. At temperatures higher than 250 K, a total of 3-4 H₂ molecules are adsorbed. In Table 5 are given the adsorption results at a mean temperature close to 300 K, which are compared with the DFT results. As it can be seen, at T = 299.97 K, the $E_{cfg} = -25.98$ kJ mol⁻¹, which is in a good agreement with the results obtained from the DFT approach, showing an average interaction energy of -3.85 kJ mol⁻¹ (a total of -26.95 kJ mol⁻¹ for coronene interacting with seven H₂ molecules), which is again reasonably close to the recent past Coupled Cluster value (CCSD(T)) of -4.71 kJ mol⁻¹ reported in Table 4. A snapshot of the final configuration of the coronene-(H₂)₇ system at T = 299.97 K is visualized in Fig. 6.

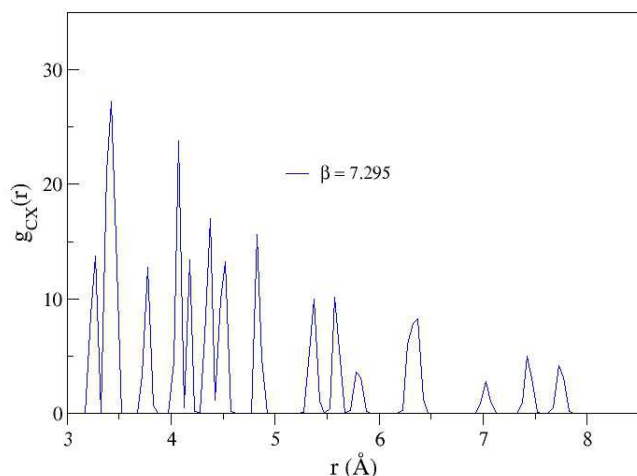


Fig. 5 The RDF, $g_{\text{C-X}}$, between a C atom and the c. m. of a H_2 molecule, defined by the symbol X, as a function of distance, r , for RNA ($\beta = 7.295$) at $T = 299.97$ K

Table 5 Adsorption of H_2 on Coronene from DFT calculations and MD simulations.

Type of calculation	# H_2 adsorbed	Distances / Å	$E_{\text{cfg}} / \text{kJ mol}^{-1}$
DFT approach	7	3.074	-26.95
MD ($T=299.97$ K)	4/7	3.065	-25.98
		3.199	
		3.179	
		3.144	

5 Conclusions

Physisorption of molecular hydrogen over graphene is very delicate because of the weak van der Waals interactions between the H_2 and graphene surface. The available computational tools to model such a system are still challenging to achieve an accurate and realistic interaction energy. This interaction has been modelled by means of a supramolecular approach for the interaction of coronene with until seven hydrogen molecules. The interaction energy, both at DFT and MD level, was evaluated taking all above facts into account. The force field (FF) fitting to the simple graphene system was imposed in a reasonably acceptable manner considering all the possible types of interactions involved in this adsorption process. For the interaction of seven hydrogen molecules with coronene, the counterpoise corrected B97-D approach shows an average interaction energy of -3.85 kJ/mol per H_2 (a total of -26.95 kJ/mol for seven H_2 's), which is reasonably close to the CCSD(T) value of -4.71 kJ/mol reported by

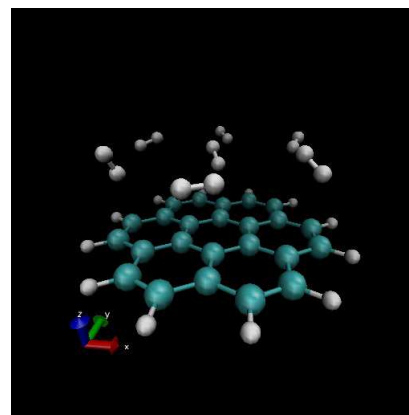


Fig. 6 Snapshot of the last configuration of the simulation for the coronene- $(\text{H}_2)_7$ system at $T = 299.97$ K. The random white-brown dumbbells are indicating the seven H_2 molecules over the white-green coronene surface.

our group. Moreover, the MD calculation reveals a mean interaction energy of -3.70 kJ/mol per H_2 (a gross mean E_{cfg} of -25.98 kJ/mol at $T = 299.97$ K), which once again is in a good agreement to the above mentioned corresponding results.

6 Acknowledgement

Part of this work was supported by the Spanish Ministerio de Economía y Competividad through project CTQ2010-19738. M. Albertí acknowledges financial support from the Ministerio de Educación y Ciencia (Spain, Project CTQ2013-41307-P) and to the Generalitat de Catalunya (2014 SGR 25). Also thanks are due to the Center de Supercomputació de Catalunya CESCA-C4 and Fundació Catalana per a la Recerca for the allocated supercomputing time. N. Faginas Lago acknowledges financial support from MIUR PRIN 2008 (contract 2008KJX4SN 003), Phys4entry FP72007-2013 (contract 242311) and EGI Inspire. Thanks are also due to INSTM, CINECA, IGI and the COMPCHEM virtual organization for the allocation of computing time. The research leading to part of the results presented in this paper has been made possible thanks to the Grid resources and services provided by the European Grid Infrastructure (EGI) and the Italian Grid Infrastructure (IGI). For more information, please reference the EGI-InSPIRE paper (<http://go.egi.eu/pdnon>) and the IGI web server (<http://www.italiagrid.it>)

References

- 1 C. Liu, M. Fan, Y.Y. and Liu, H. Cong, H. Cheng and M. Dresselhans, *Science*, 1999, **286**, 1127–1129.
- 2 Q. Wang and K. Johnson, *J. Chem. Phys.*, 1999, **110**, 577–586.

- 3 M. Hirscher, *Handbook of Hydrogen Storage: New Materials for Future Energy Storage*, Wiley-VCH, 2010.
- 4 F. Shedin, A. Geim, S. Morozov, E. Hill, P. Blake, M. Katsnelson and S. Novoselov, *Nature Materials*, 2007, **6**, 652–655.
- 5 O. Leenaerts, B. Partoens and F. Peeters, *Phys. Rev. B*, 2008, **77**, 125416(1)–125416(6).
- 6 H. Yoon, D. Jun, J. Yang, Z. Zhou and S. M.-C. C. M. Yang, *Sensors and Actuators B: Chemical*, 2011, **157**, 310–313.
- 7 G. Lu, L. Ocola and J. Chen, *Nanotechnology*, 2009, **20**, 445502(1)–445502(9).
- 8 K. Batinac, W. Yang, S. Ringer and F. Braet, *Environ. Sci. Technol.*, 2010, **44**, 1167–1176.
- 9 G. Ko, H.-Y. Kim, J. Ahn, Y.-M. Park and K. Lee, K.-Y., *Current Applied Physics*, 2010, **10**, 1002–1004.
- 10 K. Novosolov, A. Geim, S. Morozov, Y. Jiang, D.: Zhang, S. Dubonos, I. Grigorieva and A. Firsov, *Science*, 2004, **306**, 666–669.
- 11 A. Geim and K. Novoselov, *Nature Mater.*, 2007, **81**, 183–191.
- 12 A. Castro Neto, F. Guinea and N. Peres, *Rev. Mod. Phys.*, 2009, **81**, 109–162.
- 13 K. Kemp, H. Seema, M. Saleh, N. Le, K. Mahesh, V. Chandra and K. Kim, *Nanoscale*, 2013, **5**, 3149–3171.
- 14 C. Thierfelder, M. Witte, S. Blankenburg, E. Rauls and W. Schmidt, *Surface Science*, 2011, **605**, 746–749.
- 15 N. Faginas-Lago, M. Albert, A. Lagan, A. Lombardi, L. Pacifici and A. Costantini, in *Computational Science and Its Applications ICCSA 2014*, ed. B. Murgante, S. Misra, A. Rocha, C. Torre, J. Rocha, M. Falco, D. Taniar, B. Apduhan and O. Gervasi, Springer International Publishing, 2014, vol. 8579, pp. 585–600.
- 16 T. Trinh, J. Flugt, M. Hägg, D. Debeaux and S. Kjelstrup, *12th Joint European Thermodynamics Conference*, 2013, 514–518.
- 17 D.-E. Jiang and Z. C. (Eds.), *Graphene Chemistry: Theoretical Perspectives*, Springer-Verlag, John Wiley & Sons, 2013.
- 18 J. Petucci, C. LeBlond, M. Karimi and G. Vidali, *J. Chem. Phys.*, 2013, **139**, 044606(1)–044706(12).
- 19 G. Vidali, *J. Low. Temp. Phys.*, 2013, **170**, 1–30.
- 20 Y. Okamoto and Y. Miyamoto, *J. Phys. Chem. B*, 2001, **105**, 3470.
- 21 Y. Okamoto and Y. Miyamoto, *J. Chem. Phys.*, 2005, **122**, 104709.
- 22 S. Patchkovskii, J. S. Tse, S. N. Yurchenko, L. Zhechkov, T. Heine and G. Seifert, *PNAS*, 2005, **102**, 10439.
- 23 O.-E. H. J.-M. Simon and S. Kjelstrup, *J. Phys. Chem. C*, 2010, **114**, 10212.
- 24 S. Attinger and P. K. (Eds.), *Lecture Notes in Computational Science and Engineering: Multiscale Modelling and Simulation*, Springer-Verlag, Berlin, 2004.
- 25 P. Pirani, S. Brizi, L. Roncaratti, P. Casavecchia, D. Cappelletti and F. Vecchiocattivi, *Phys. Chem. Chem. Phys.*, 2008, **10**, 5489.
- 26 N. Faginas-Lago, F. Huarte Larrañaga and M. Albertí, *Eur. Phys. J. D*, 2009, **55**, 75.
- 27 M. Albertí, A. Costantini, A. Laganà and F. Pirani, *J. Phys. Chem. B*, 2012, **116**, 4220–4227.
- 28 M. Albertí, A. Aguilar, J. M. Lucas and F. Pirani, *Theor. Chem. Acc.*, 2009, **123**, 21–27.
- 29 M. Albertí, A. Aguilar, D. Cappelletti, A. Laganà and F. Pirani, *Int. J. Mass Spec.*, 2009, **280**, 50–56.
- 30 A. D. Becke, *J. Chem. Phys.*, 1993, **98**, 5648.
- 31 R. D. W.J. Hehre and J. Pople, *J. Chem. Phys.*, 1972, **56**, 2257.
- 32 M. J. Frisch, G. W. Trucks, H. B. Schlegel, G. E. Scuseria, M. A. Robb, J. R. Cheeseman, V. B. G. Scalmani, B. Mennucci, G. A. Petersson, H. Nakatsuji, M. Caricato, X. Li, H. P. Hratchian, A. F. Izmaylov, J. Bloino, G. Zheng, J. L. Sonnenberg, M. Hada, M. Ehara, K. Toyota, R. Fukuda, J. Hasegawa, M. Ishida, T. Nakajima, Y. Honda, O. Kitao, H. Nakai, T. Vreven, J. A. Montgomery, J. J. E. Peralta, F. Ogliaro, M. Bearpark, J. J. Heyd, E. Brothers, K. N. Kudin, V. N. Staroverov, T. Keith, R. Kobayashi, J. Normand, K. Raghavachari, A. Rendell, J. C. Burant, S. S. Iyengar, J. Tomasi, M. Cossi, N. Rega, J. M. Millam, M. Klene, J. E. Knox, J. B. Cross, V. Bakken, C. Adamo, J. Jaramil-loa, R. Gomperts, R. E. Stratmann, O. Yazyev, A. J. Austin, R. Cammi, C. Pomelli, J. W. Ochterski, R. L. Martin, K. Morokuma, V. G. Zakrzewski, G. A. Voth, P. Salvador, J. J. Dannenberg, S. Dapprich, A. D. Daniels, O. Farkas, J. B. Foresman, J. V. Ortiz, J. Cioslowski, and D. J. Fox, *Gaussian09 Revision D.01*, Gaussian Inc. Wallingford CT 2009.
- 33 S. F. Boys and F. Bernardi, *Mol. Phys.*, 1970, **19**, 553.
- 34 S. Grimme, *J. Comput. Chem.*, 2006, **27**, 1787.
- 35 C. H. A. Schaefer and R. Ahlrichs, *J. Chem. Phys.*, 1994, **100**, 5829.
- 36 F. Tran, J. Weber, T. Wesolowski, F. Cheikh, Y. Ellinger and F. Pauzat, *J. Phys. Chem. B*, 2002, **106**, 8689.
- 37 J. Murrell and K. Sorbie, *J. Chem. Soc. Faraday Trans. II*, 1974, **70**, 1552.
- 38 P. M. Morse, *Phys. Rev.*, 1929, **34**, 57–64.
- 39 W. Smith, C. Yong and P. Rodger, *Molecular Simulation*, 2002, **28**, 385–471.